CHAPTER – 3

SOFTWARE IMPLEMENTATION OF ALGORITHM FOR RDC USING ARCTANGENT TECHNIQUE

CHAPTER – 3

SOFTWARE IMPLEMENTATION OF ALGORITHM FOR RDC USING ARCTANGENT TECHNIQUE

The aim of the following chapters is systematically review the mathematical models of the two mainly used algorithms for the design of resolver to digital converters, namely Arctangent technique and ATO, before proceedings to the design and observation algorithms for them. The measurement of rotor shaft angular position with the above two algorithms are studied through simulation. All the analysis and control algorithms presented in later chapters are based on these two models.

3.1 INTRODUCTION:

The measurement of the initial rotor position at standstill has to be achieved to gain the maximum starting torque. The resolver is a sensor that satisfies this condition along with the fact that it is a reliable and robust device for severe environments. The resolvers are basically rotating transformers. It has a rotating coil placed in the rotor that is fed by a high frequency sinusoidal voltage and two stator coils placed in the quadrature. Once the rotor is excited by a high frequency sinusoidal source, the induced voltages would be developed on the stator coils. The amplitude of these stator coils are modulated with the rotor position. The demodulation and filtering techniques have to be designed to extract the angular position of the rotor [1–3].

The accuracy achieved in speed and/or position measurement by the resolvers depends on the quality of the analog signals and on the resolution of the digital converters used to interface resolvers to the control units. This conversion is made by RDCs. RDC is an Integrated Circuit (IC) that can be easily mounted on the motion

control board and is used to demodulate the two resolver output signals. The RDC IC was designed to calculate the error between actual angle and computed angle. This angular position error is controlled to zero, resulting in the computed angle converge to the actual one [4–6]. The main drawback of RDC IC is its cost which is same price as that of the resolver [7]. However, the price of the specific IC module is high, and the weight and power dissipation are large, therefore increasing the cost of the whole system which limits the usage of its application.

In order to avoid the use of these RDCs, more and more attention has been focussed on the design of software based RDCs and ways to improve the measurement accuracy [8-16]. Making instrument intelligent is a trend in the new control system which means more hardware is substituted by software.

The problem described above and addressed in this thesis is actually a series of sub problems. In the present work, the design of software based RDC for single speed resolver using two algorithms is well addressed and successfully simulated in MATLAB® SIMULINK®. The developed two algorithms are:

i) Arctangent or Inverse Tangent or Direct angle technique

ii) Angle Tracking Observer algorithm

3.2 MATHEMATICAL MODEL OF ARCTANGENT TECHNIQUE BASED RDC

The block schematic of angle extraction using Arctangent algorithm is shown in Figure 3.1. The resolver secondary signals represent the SIN and COS of the rotor angle, the ratio of the signal amplitudes is the tangent of the rotor angle. Thus the rotor angle, θ is the arctangent of the SIN signal divided by the COS signal.

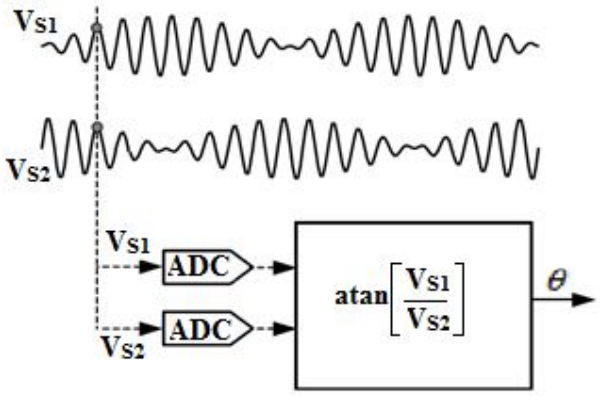

Figure 3.1 Angle extraction using Arctangent algorithm

$$\theta = \arctan\left(\frac{Sin(\theta)}{Cos(\theta)}\right) \qquad (3.1)$$

The block diagram of the proposed RDC scheme using Arctangent algorithm is shown in Figure 3.2.

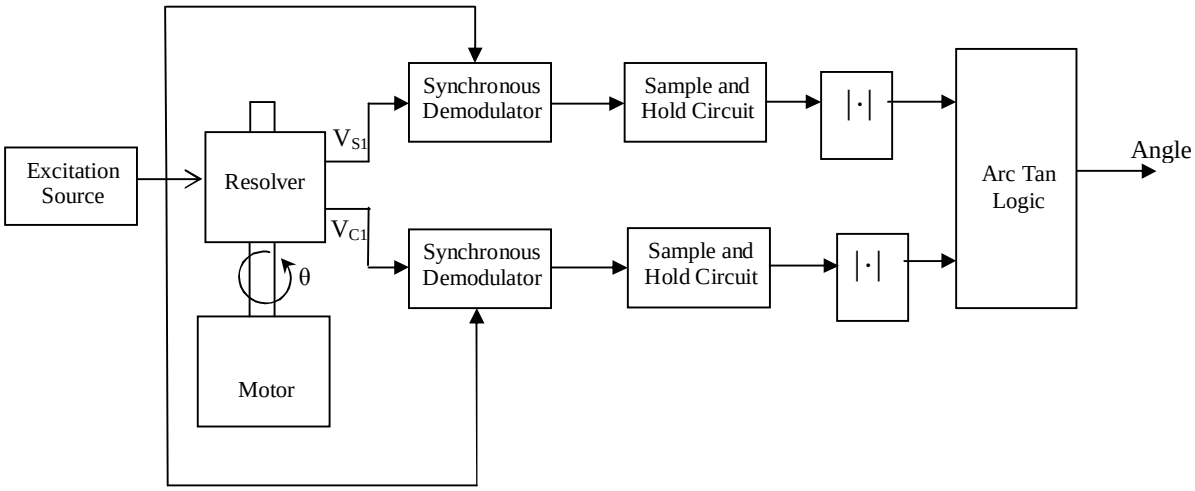

Figure 3.2 Arctangent algorithm based RDC

The resolver is excited by either sinusoidal or square wave signal with a fixed frequency. If sinusoidal signal is used as excitation signal, it is difficult to detect the adequate sampling moments of the output signals of the resolver because of the phase shift between the input and output signals. If the resolver is excited by a square wave signal then the output signals will be flat extremes that allow having an interval of time for sampling the output. For this reason, the square wave signal is preferred as excitation signal to excite the resolver. One more advantage of using square wave as an excitation signal is that the generation of square wave signal is easier than generating a sinusoidal signal for a processor. So, in the proposed design, square wave signal is chosen as an excitation signal to excite the resolver.

3.2.1 Mathematical Model of the Proposed Arctangent algorithm

For the purpose of understanding and designing of RDC based on Arctangent algorithm, it is necessary to know the mathematical model of resolver and RDC based on Arctangent algorithm. In the proposed design, the resolver is excited with a square wave signal but, for easy mathematical modelling, sine wave is considered as excitation signal, V_{REF} of peak to peak amplitude 1 Volt with variable frequency of 1 Hz to 5 kHz. The mathematical expression for the excitation signal is given as

$$V_{REF} = Sin(2\pi\ f_e t) \qquad (3.2)$$

The reference signal, V_{REF} modulates the SIN and COS functions of rotor shaft angles. The resolver produces two amplitude modulated signals, V_{S1} and V_{C1}, as outputs. Generally, the excitation frequency (f_e) of the rotor excitation is higher than the rotation angular frequency (f_m). So the modulated output signals of the resolver are given as

$$V_{S1} = \alpha\, Sin(2\pi\, f_e t) \cdot Sin(\theta) \qquad (3.3)$$

$$V_{C1} = \alpha\, Sin(2\pi\, f_e t) \cdot Cos(\theta) \qquad (3.4)$$

Where ' α ' is the resolver transformation constant and is assumed as one. The value of $\theta = 2\pi\, f_m t.$ The rotation frequency, (f_m) is calculated depending upon the speed of the motor attached to the resolver and is also known as revolution of the resolver in one second. For example, if the motor speed is 600rpm then the rotation frequency, f_m is given as

$$f_m = \frac{600 rpm}{60} = 10\, Hz \qquad (3.5)$$

The output signals of the resolver are Double Side Band Suppressed Carrier (DSB-SC) signals. The synchronous demodulator is mostly used DSB-SC demodulation method. In synchronous demodulation method, the same excitation signal is used to remove the excitation signal presented in the outputs of the resolver. The block diagram of synchronous demodulator is shown in Figure 3.3.

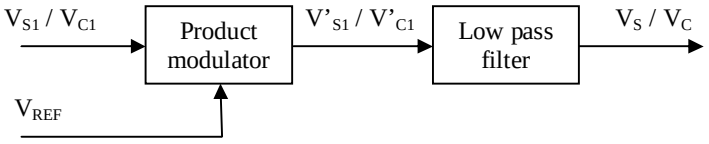

Figure 3.3 Synchronous demodulator

Product modulator takes either V_{S1} or V_{C1} as one input and V_{REF} as second input and gives the product of the two inputs as output. The mathematical representation of the output of the product modulator for $\alpha = 1$ is given as

$$\begin{aligned} V'_{S1} &= V_{S1} \cdot V_{REF} \\ &= Sin(2\pi\ f_e t) \cdot Sin(\theta) \cdot Sin(2\pi f_e t) \\ &= \left\{ \frac{1}{2} - \frac{1}{2} Cos(4\pi\ f_e t) \right\} \cdot Sin(\theta) \end{aligned} \qquad (3.6)$$

Similarly

$$\begin{aligned} V'_{C1} &= V_{C1} \cdot V_{REF} \\ &= Sin(2\pi\ f_e t) \cdot Cos(\theta) \cdot\ Sin(2\pi f_e t) \\ &= \left\{ \frac{1}{2} - \frac{1}{2} Cos(4\pi\ f_e t) \right\} \cdot Cos(\theta) \end{aligned} \qquad (3.7)$$

The product modulator outputs as in (3.6) and (3.7) are with a high frequency excitation signal and these frequencies need to be removed to measure the rotor angle, θ. In order to remove the high frequency carrier signal, the two product modulated output signals, V'_{S1} and V'_{C1} are passed through a low pass filer with a higher cut-off frequency equal to the rotational frequency, f_m.

The outputs of the two low pass filters are

$$V_S = \frac{1}{2} Sin(\theta) \qquad (3.8)$$

and

$$V_C = \frac{1}{2} Cos(\theta) \qquad (3.9)$$

The low pass filter outputs as in (3.8) and (3.9) contain only the angular position information of the resolver rotor. So, to measure the angle for every instant of time, the two signals must be sampled. The instantaneous samples of the signals in (3.8) and (3.9) are obtained by sampling the signals for every rising edge of the excitation frequency. The block diagram of sample and hold circuit is given in Figure 3.4.

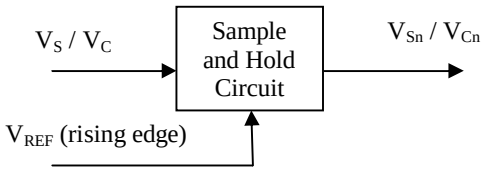

Figure 3.4 Sample and hold circuit

The sampled signals of (3.8) and (3.9) are given as

$$V_{Sn} = \frac{1}{2} Sin(\theta_n) \qquad (3.10)$$

and

$$V_{Cn} = \frac{1}{2} Cos(\theta_n) \qquad (3.11)$$

The SIN and COS envelopes obtained after sample and hold circuit, as in (3.10) and (3.11) are used to compute the rotor angular position. The two sampled signals are fed to an absolute circuit in order to get the linearity. The computed rotor shaft angular position is given as

$$\theta = \arctan\left[\frac{|V_{Sn}|}{|V_{cn}|}\right] = \arctan\left[\frac{|Sin(\theta_n)|}{|Cos(\theta_n)|}\right] \qquad (3.12)$$

3.3 METHODOLOGY

Based on the theory, mathematical representation and information; the overall system of the Arctangent based RDC as shown in Figure 3.2 is implemented in the MATLAB® SIMULINK® and is shown in Figure 3.5. This model is only based on theory and is ideal without any limitations.

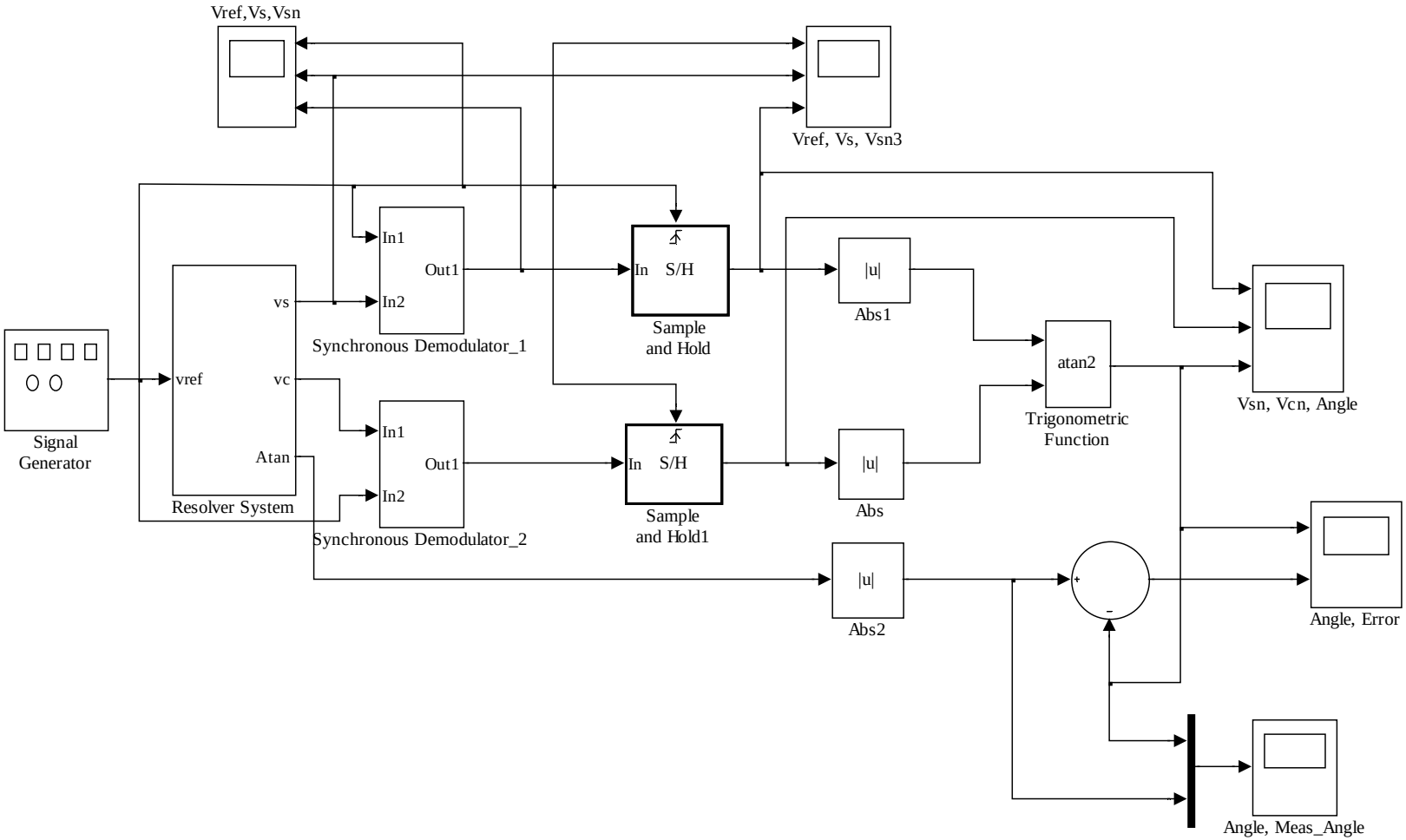

Figure 3.5 MATLAB® SIMULINK® model of RDC using Arctangent algorithm

The resolver block in Figure 3.5 consists of the excitation signal as input and the modulated sinusoidal output signals. It is possible to add errors such as amplitude imbalance and imperfect quadrature. Differences in amplitude of the modulated output signals results in amplitude imbalance and a phase shift that is not exactly 90^0 results in imperfect quadrature [17].

The main blocks of the implemented RDC model are

i) Synchronous demodulator

ii) Sample and hold circuit

iii) Absolute value circuit

iv) Arctangent logic circuit

The excitation signal generator feeds the high frequency excitation signal to the resolver. When the resolver rotor is rotated, it induces the two amplitude modulated signals. These two modulated signals have to be demodulated to obtain the rotor angular position from the resolver. For the simulation, the resolver transformation constant is chosen as one.

Synchronous demodulator is used to demodulate the outputs signals of the resolver system and is designed with a product modulator followed by a low pass filter, as shown in Fig 3.3. The magnitude and phase responses of the low pass filter are shown in Figure 3.6.

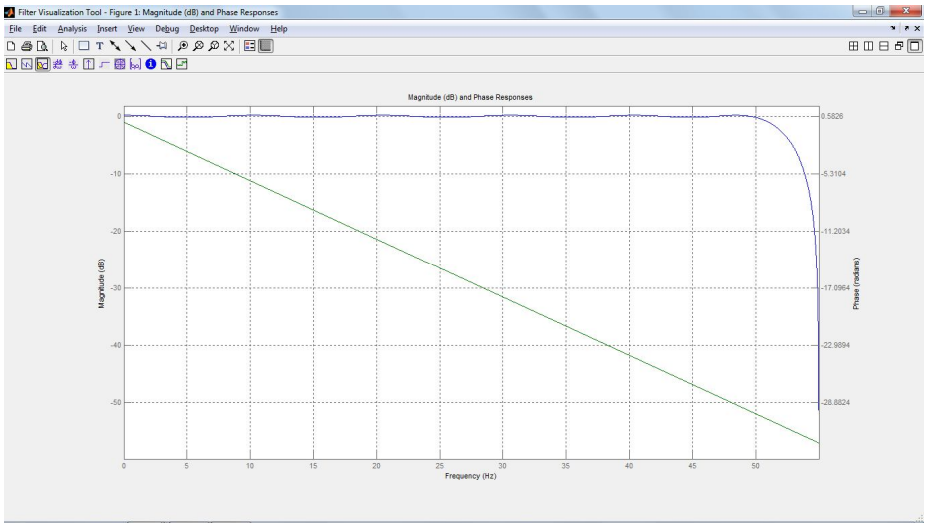

Figure 3.6 Frequency response of low pass filter

The two demodulated signals are applied to the sample and hold circuits and are simultaneously sampled at the zero crossing of the excitation signal to avoid any delay in the extracted sin-cosine envelopes. So, the detection of zero crossing of excitation signal plays an important role in the accuracy of the resolver.

The high frequency component in (3.7) is filtered by the low pass filter and it passes only the rotational frequency. The output of this low pass filter is sampled with rising edge of the excitation frequency and the instantaneous absolute value is taken using an absolute circuit. The signals in (3.10) and (3.11) are given as input to atan2 block to measure the rotor shaft angular position of the resolver.

3.4 RESULTS AND DISCUSSIONS

The MATLAB® SIMULINK® model of RDC using Arctangent algorithm is built and is shown in Figure 3.5. Computer simulations have been performed to evaluate the tracking performance of the proposed scheme and to examine the RDC system.

MATLAB® SIMULINK® is used as the simulation platform. The simulation parameters of MATLAB® SIMULINK® are given in Table 3.1.

Table 3.1 Simulation parameters of MATLAB® SIMULINK®

Solver Type: Variable step	Solver: Ode45 (Dormant Prince)
Maximum step size: 1e–6	Relative Tolerance: 1e–3
Minimum step size: auto	Absolute tolerance: auto
Initial step size: 1e–6	Time tolerance: 10x128xeps

The performance of the proposed RDC model is investigated for different cases. For the simulation, the resolver is initially excited with a square wave signal of 1 Volt peak to peak amplitude with a frequency of 5 kHz at a sampling rate of 100 kHz.

Case (i): When the resolver rotor speed is 300 rpm

The simulation results of the proposed RDC model for the rotor speed of 300 rpm i.e. 5 Hz are shown from Figure 3.7 to Figure 3.11. Figure 3.7 shows the square wave excitation signal, modulated SIN and COS signals from resolver.

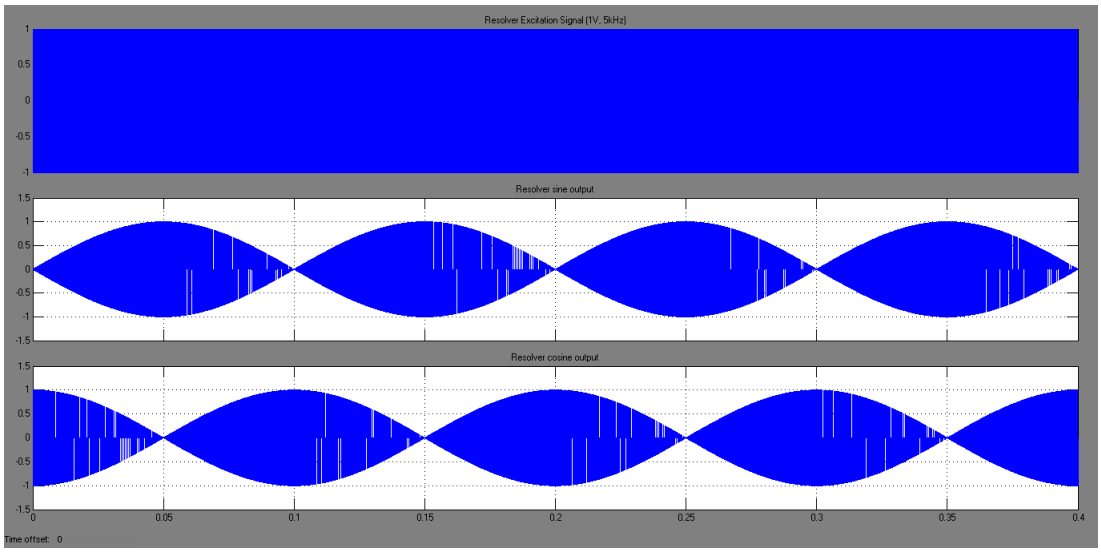

Figure 3.7 Square wave excitation signal, SIN and COS outputs of the resolver

The SIN and COS modulated signals of the resolver are demodulated by the synchronous detector and are shown in Figure 3.8. The sample and hold circuits sampled the demodulated signals with a sampling frequency of excitation signal and these sampled signal are used to compute the rotor shaft position. The sampled demodulated signals and computed mechanical angle are shown in Figure 3.9.

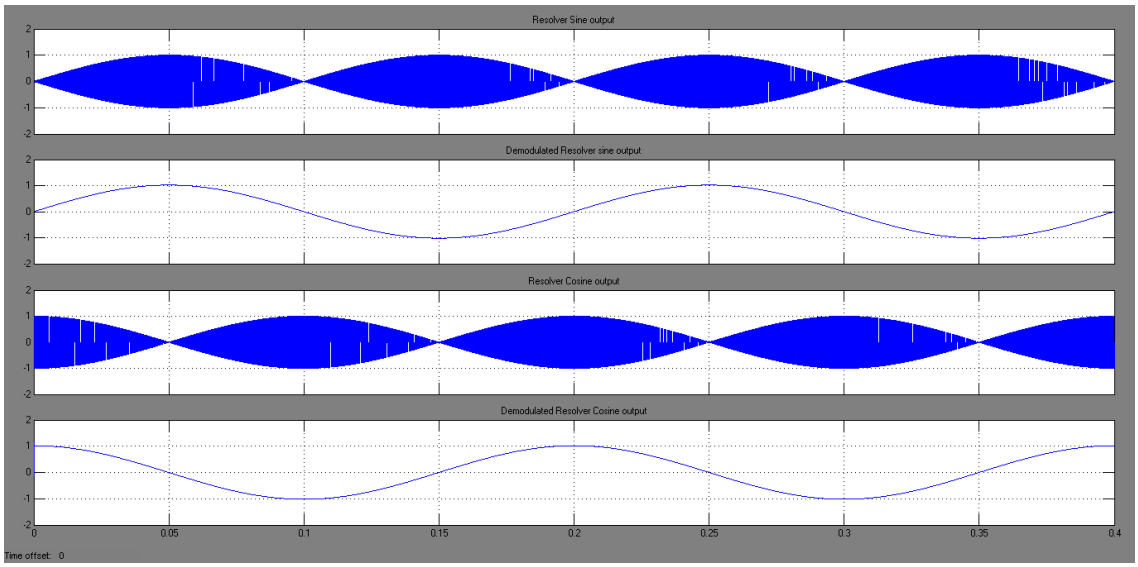

Figure 3.8 SIN output, demodulated SIN, COS output and demodulated COS signals

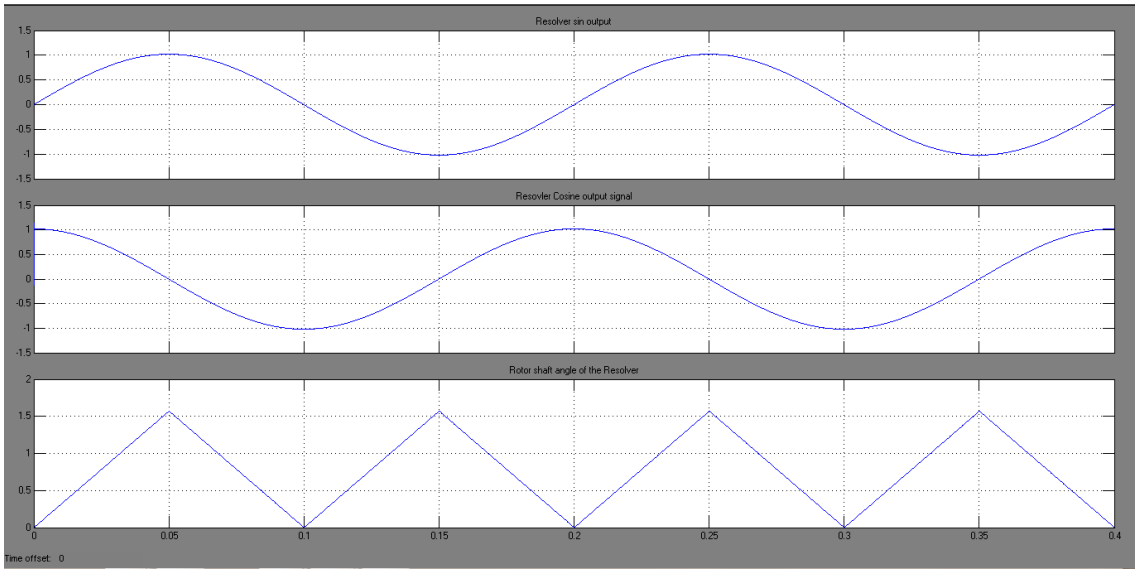

Figure 3.9 Sampled SIN and COS outputs and measured rotor shaft angle

The actual rotor shaft angle and measured angle of the proposed RDC model are shown in Figure 3.10. In this case, the actual and estimated rotor position angles almost overlap together with very small error (0.0093^0). Figure 3.11 shows the measured rotor angle and the error between the actual angle and the measured rotor angle. The maximum error between the actual rotor angle and measured rotor angle of this RDC using Arctangent algorithm is 0.0093^0 when the rotor is operating with a speed of 300 rpm.

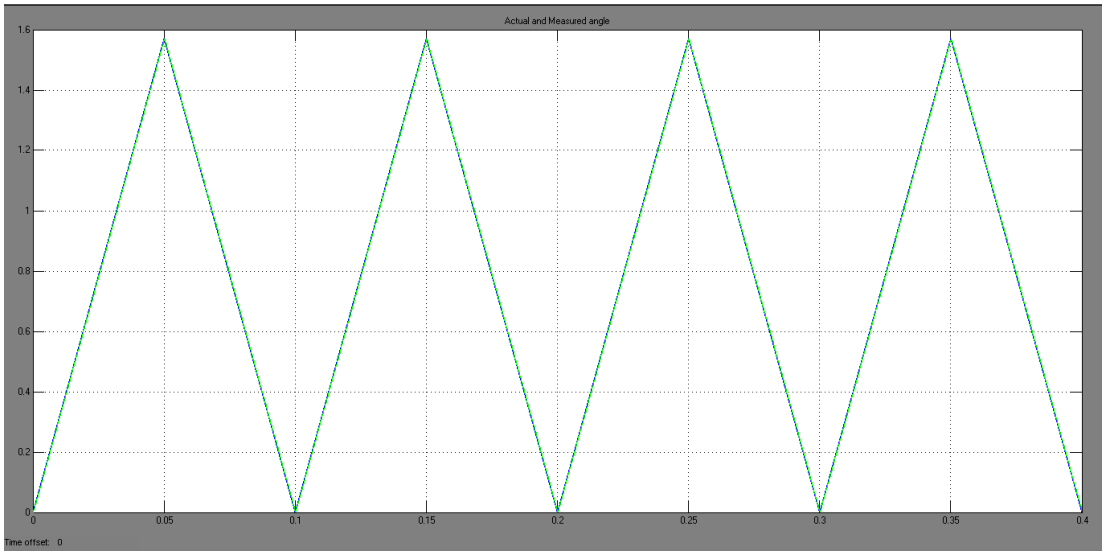

Figure 3.10 Actual rotor angle (blue) and measured rotor angle (green)

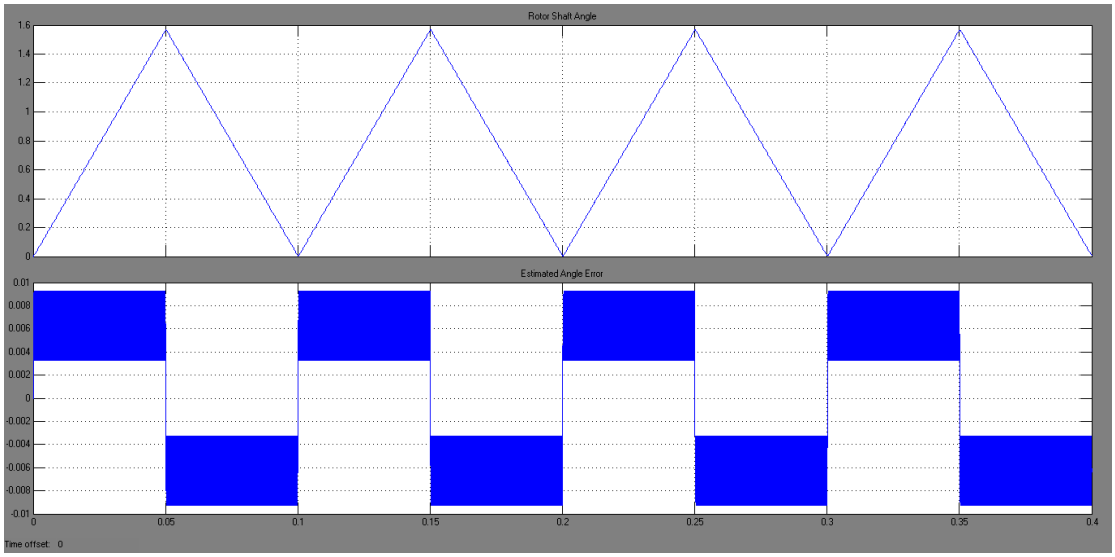

Figure 3.11 Measured rotor angle and rotor angle error

Case (ii): When the resolver rotor speed is 600 rpm:

The simulation results of the proposed RDC model when the rotor shaft is running at 600 rpm are shown from Figure 3.12 to Figure 3.16. Figure 3.12 shows the excitation signal, modulated SIN and COS signals from resolver. The modulated resolver signals and their demodulated signals are presented in Figure 3.13.

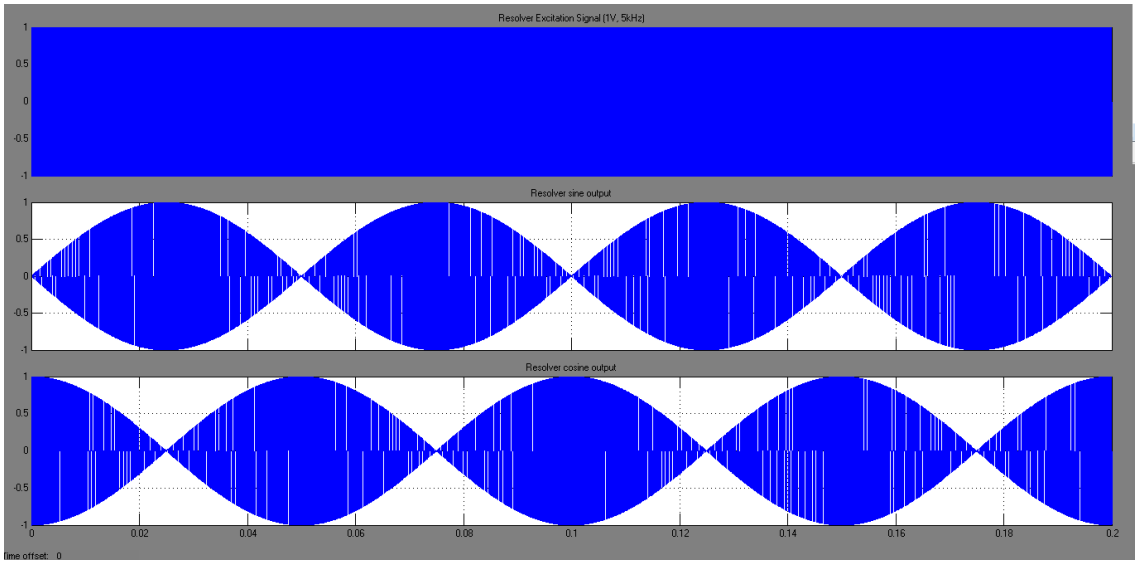

Figure 3.12 Square wave excitation signal, SIN and COS outputs of the resolver

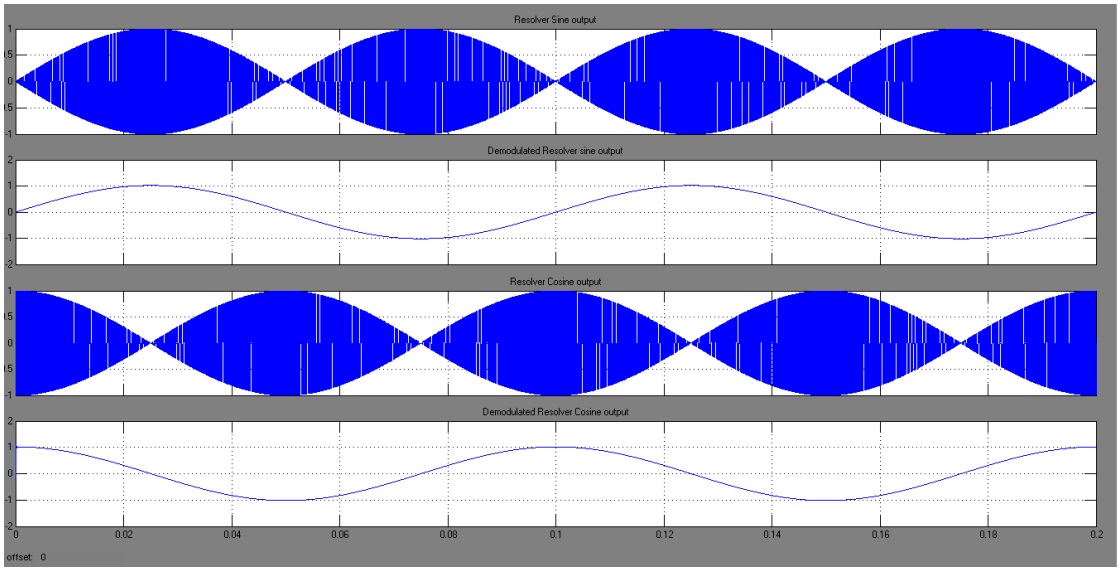

Figure 3.13 SIN output, demodulated SIN, COS output and demodulated COS signals

Figure 3.14 shows the sampled demodulated signals of the resolver and the measured rotor mechanical angle. The actual rotor shaft angle and measured angle of the proposed RDC model are shown in Figure 3.15 and both waveforms almost overlap together with very small error (0.0185^0). The measured rotor angle and the error between the actual angle and the measured rotor angle are shown in Figure 3.16. The maximum rotor angular error is 0.0185^0 when the rotor is operating with a speed of 600 rpm.

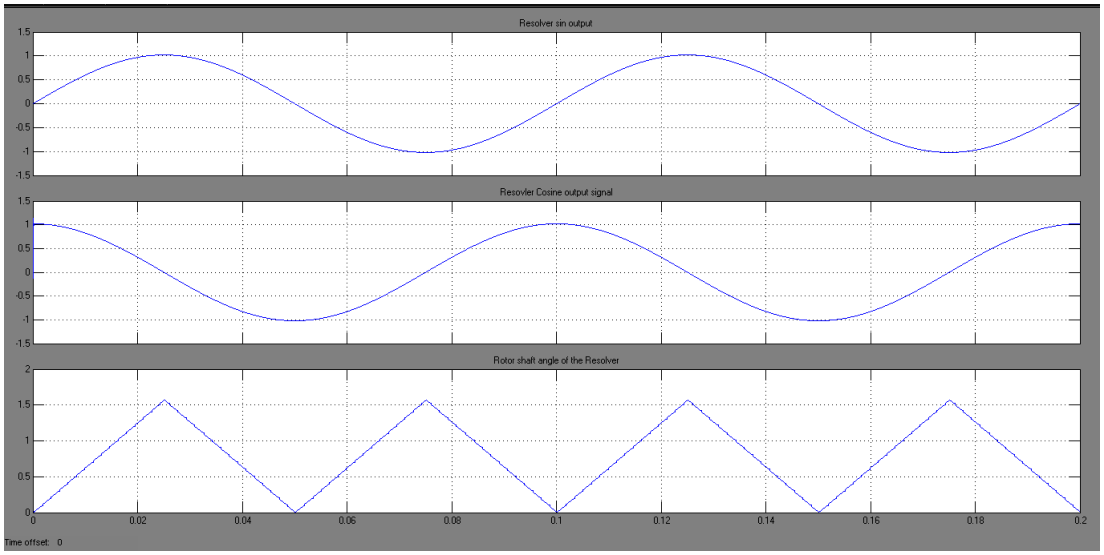

Figure 3.14 Sampled SIN and COS outputs and measured rotor shaft angle

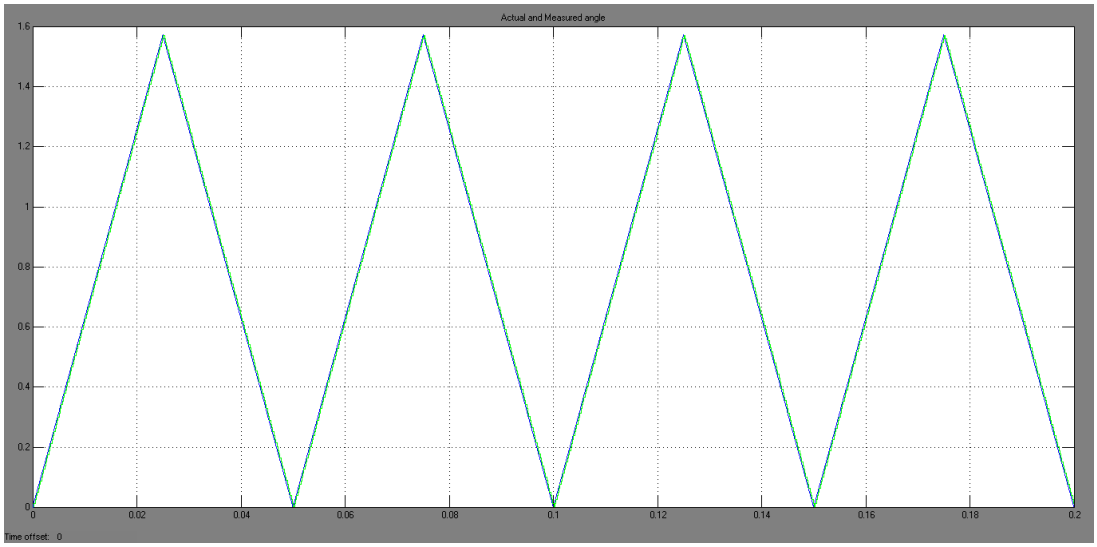

Figure 3.15 Actual rotor angle (blue) and measured rotor angle (green)

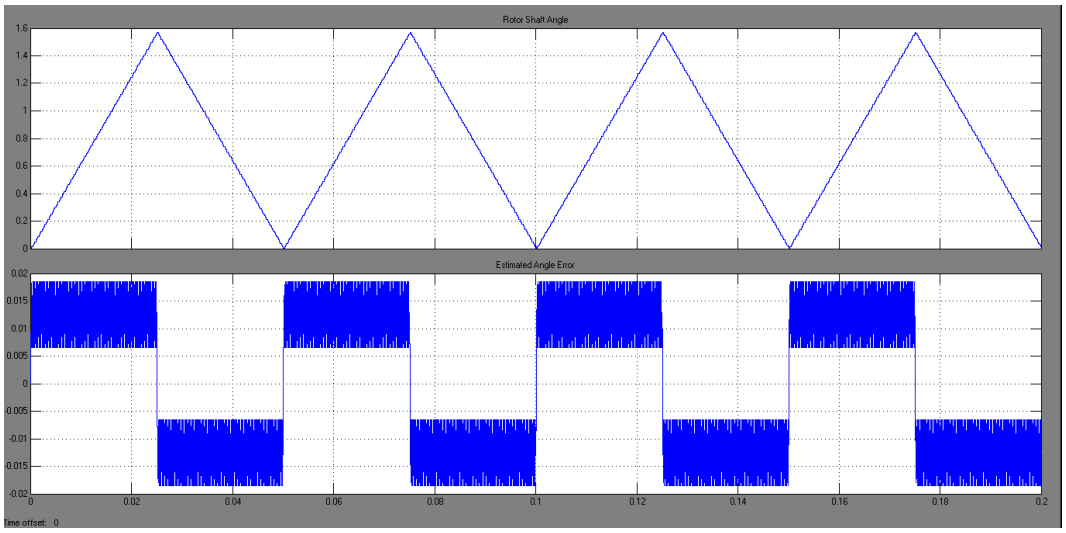

Figure 3.16 Measured rotor angle and rotor angle error

From the above simulation results, as presented in Figure 3.11 and Figure 3.16, it is noticed that the maximum measured angular position error is 0.0093^0 and 0.0185^0 for the rotor speed of 300 rpm and 600 rpm respectively. From Figure 3.10 and Fig 3.15, it is observed that the estimated rotor position angle tracks the real one with small amount of error.

Case (iii): When the resolver rotor speed is 3000 rpm:

The simulation results when the rotor shaft is running at 3000 rpm are shown from Figure 3.17 to Figure 3.21.

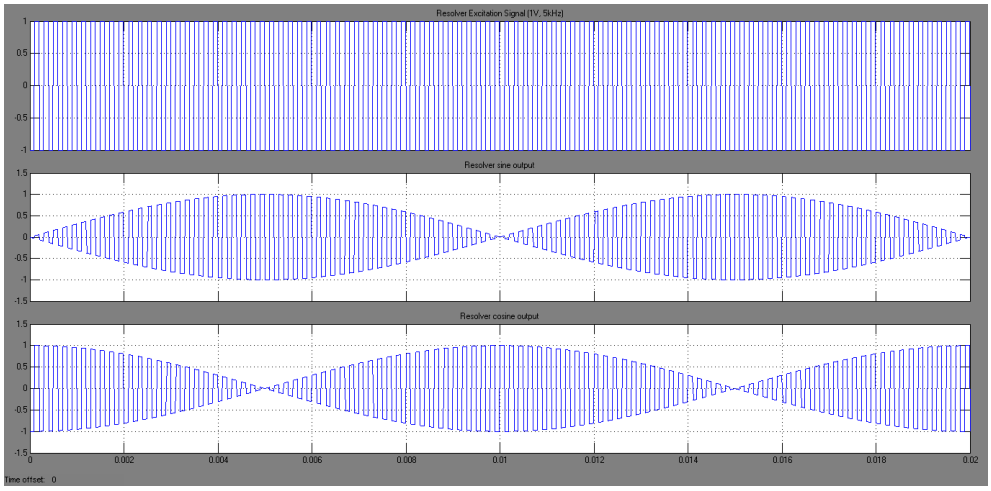

Figure 3.17 Square wave excitation signal, SIN and COS outputs of the resolver

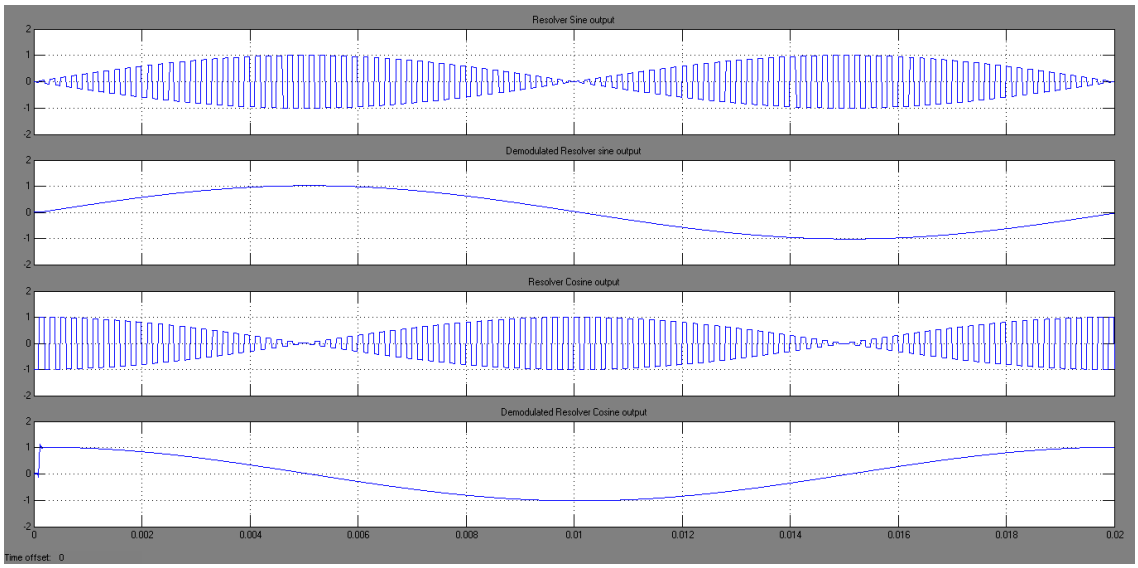

Figure 3.18 SIN output, demodulated SIN, COS output and demodulated COS signals

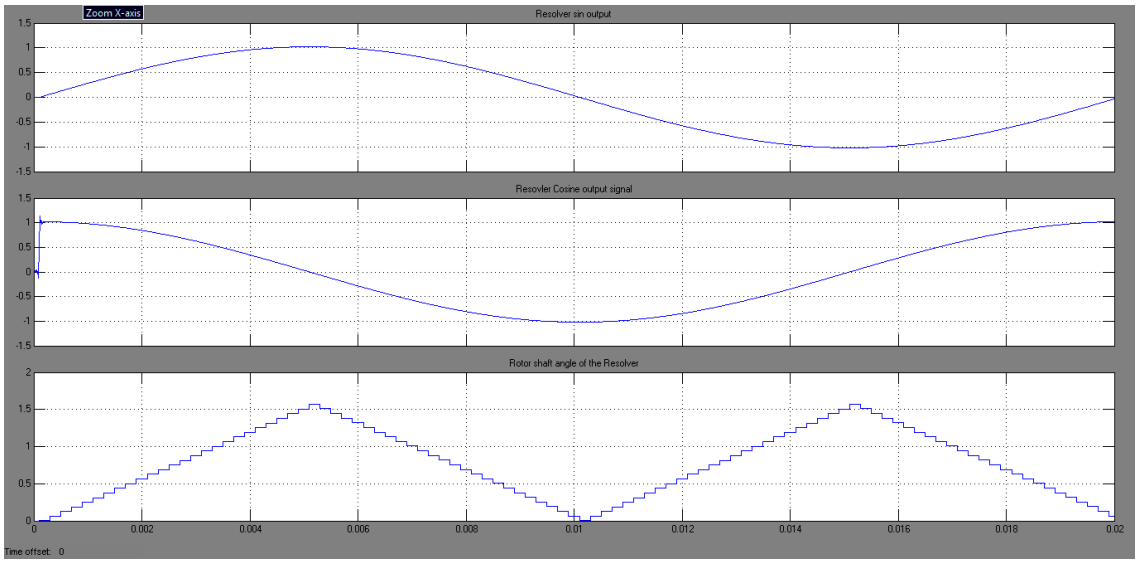

Figure 3.19 Sampled SIN and COS outputs and measured rotor shaft angle

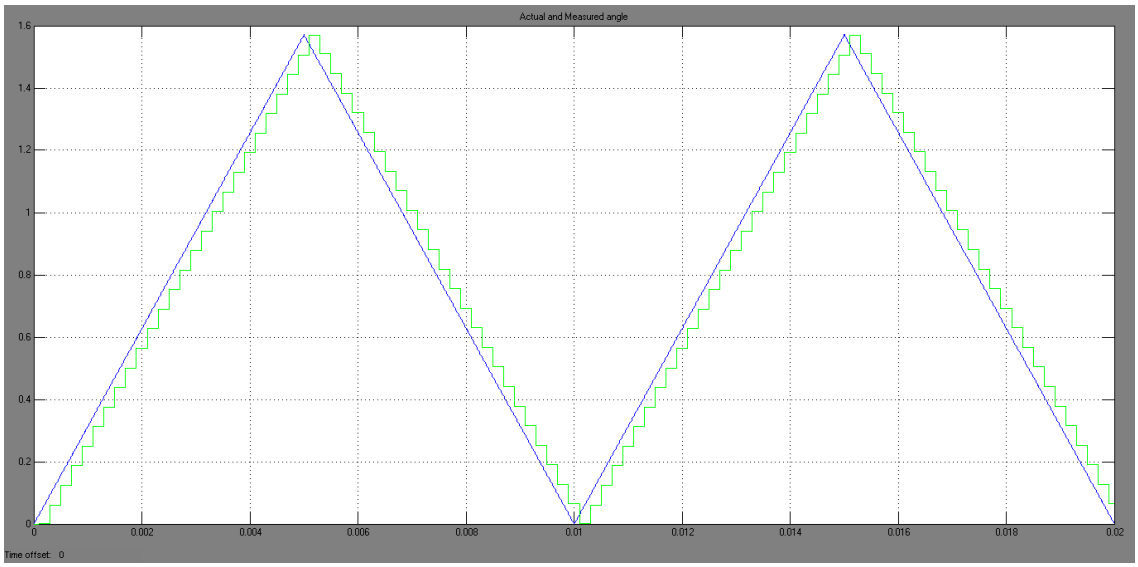

Figure 3.20 Actual rotor angle (blue) and measured rotor angle (green)

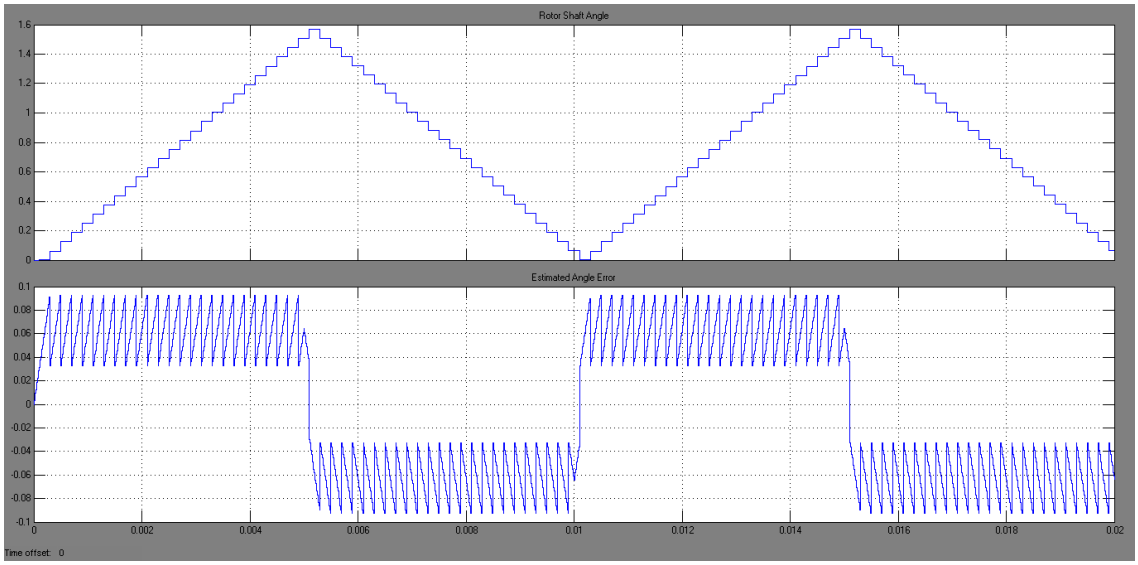

Figure 3.21 Measured rotor angle and rotor angle error

From the above simulation results, as presented in Figure 3.21, it is noticed that the maximum measured angular position error is 0.0927^0 for the rotor speed of 3000 rpm. From Figure 3.11, Figure 3.16 and Figure 3.21, it is also observed that as the speed of the rotor shaft increases the amount of estimated angle position error is also increased.

The performance of the proposed RDC model is verified for different speeds starting from 300 rpm to 3600 rpm. Table 3.2 gives the measured rotor angular position error for different speeds. From Table 3.2, it is observed that the RDC using Arctangent algorithm gives a negligible amount of rotor angle error when the speed is less than 600 rpm, and as the speed of the rotor increases the angle error is also increased. The graph between rotor shaft angular position error and rotor speed is shown in Figure 3.22.

Table 3.2 Rotor angular position error for different speeds

S.No	**Rotor Speed in rpm**	**Rotor angle error in degrees**
1	300	0.0093
2	600	0.0185
3	900	0.0278
4	1200	0.0371
5	1500	0.0463
6	1800	0.0556
7	2100	0.0649
8	2400	0.0741
9	2700	0.0834
10	3000	0.0927
11	3600	0.1112

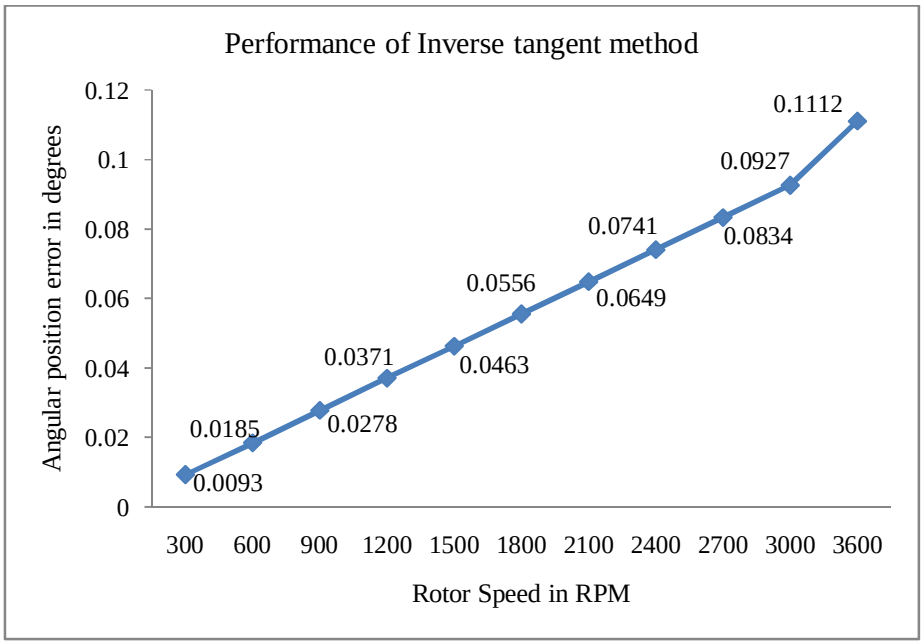

Figure 3.22 Graph between rotor angular position error and rotor speed

3.5 CONCLUSION:

The angular position is a very important parameter to know the right position of the rotor shaft and for efficient control of the motor at all time. Arctangent algorithm is an open loop method, thus the angular position of the rotor shaft of the proposed RDC using Arctangent algorithm is measured without any tracking of the past positions. The error of the measured rotor shaft angle of the resolver is very small and is negligible at lower speeds, but the error is high at higher speeds. So, this algorithm may not provide high angle accuracy but it provides good precision at low rotor speed i.e. less than 600rpm.

REFERENCES

[1]. Anna K S Baasch, Elisabeth C Lemos, Felipe Stein, Aleksander S Paterno, José de Oliveira and Ademir Nied, "Resolver-to-digital conversion implementation–a filter approach to PMSM position measurement," *in proceedings of IEEE 2011 International Conference on Power Engineering, Energy and Electrical Drives*, May 2011, Spain.

[2]. Weera Kaewjinda and Mongkol Konghirun, "Vector Control Drive of Permanent Magnet Synchronous Motor using Resolver Sensor," *ECTI Transactions on Electrical Engineering, Electronics, and Communications*, Vol.5, No.1, pp. 134-138, February 2007.

[3]. Mongkol Konghirun, "A Resolver-Based Vector Control Drive of Permanent Magnet Synchronous Motor on a Fixed-Point Digital Signal Processor," *IEEE transactions on TENCON 2004*, Vol. 4, pp. 167-170, November 2004.

[4]. Prerna Gaur, Sumit Bhardwaj, Naveen Jain, Nipun Garg, Prashant A, A. P.Mittal, and Bhim Singh, "A novel method for extraction of speed from resolver output using neural network in vector control of PMSM," *in proceedings of IEEE 2011*, 2011.

[5]. Ned Mohan, "First Course on Power Electronics and Drives," MNPERE, 2005.

[6]. Prerna Gaur, "Intelligent Motion Control on Permanent Magnet AC Motors," *Division of Instrumentation and Control*, NSIT, Delhi, May, 2009.

[7]. Ciro Attaianese and Giuseppe Tomasso, "Position measurement in industrial drives by means of low-cost resolver-to-digital converter," *IEEE Transactions on Instrumentation and Measurement*, Vol. 56, No. 6, pp. 2155-2159, December 2007.

[8]. Duane C. Hanselman, "Techniques for Improving Resolver-to-Digital Conversion Accuracy," *IEEE Transactions on Industrial Electronics*, Vol. 38, No. 6, pp. 501-504, December 1991.

[9]. Choong-Hyuk Yim, In-Joong Ha and Myoung-Sam KO, "A resolver-to-digital conversion method for fast tracking," *IEEE Transactions on Industrial Electronics*, Vol. 39, No. 5, pp. 369–378, 1992.

[10]. *C.* Attaianese, *G.* Tomasso and D. DeBonis, "A low cost resolver-to-digital converter**,**" *in proceedings IEEE International Electrical Machine Drives Conference*, Cambridge, MA, June 2001, pp. 917–921.

[11]. Mohieddine Benammar, Lazhar Ben-Brahim, and Mohd A. Alhamadi, "A novel resolverto-360^0 linearized converter," *IEEE Sensors Journal*, Vol. 4, No.1, pp. 96–101, 2004.

[12]. Mohieddine Benammar, Lazhar Ben-Brahim, and Mohd A. Alhamadi, "A high precision resolver-to-DC converter," *IEEE Transactions on Instrumentation and Measurement*, Vol. 54, No. 6, pp. 2289-2296, December, 2005.

[13]. Aengus Murray, Bruce Hare and Akihiro Hirao, "42.3: Resolver position sensing system with integrated fault detection for automotive applications," *in proceedings of IEEE International Conference*, 2002, pp. 864-869.

[14]. A.V.Radun, and M.Seshadri, "A Programmable Logic Device Resolver Simulator [for motor control]," *in Proceedings of IEEE Southeastcon*, 1999, Vol. 1, pp. 159-164.

[15]. Duane Hanselman, "Resolver signal requirements for high accuracy resolver-to-digital conversion," *in proceedings of IEEE International Conference, 1989,* pp. 486-493.

[16]. S. Sarma, V.K. Agrawal and S. Udupa, “Software-based resolver-to-digital conversion using a DSP”, *IEEE Transactions on Industrial Electronics*, Vol. 55, No. 1, pp.371-379, January 2008.

[17]. S. H. Hwang, H. J. Kim, J. M. Kim, Hui Li and Liming Liu, “Compensation of amplitude imbalance and imperfect quadrature in resolver signals for PMSM drives,” *in proceedings of IEEE 2009*, pp. 1720-1725.